Bergische Universität Wuppertal

Fachbereich Mathematik und Naturwissenschaften

Lehrstuhl für Angewandte Mathematik
und Numerische Mathematik

Preprint BUW-AMNA 06/06

Roland Pulch

Initial-boundary value problems of warped MPDAEs including minimisation criteria

October 2006

http://www.math.uni-wuppertal.de/org/Num/

Initial-boundary value problems of warped MPDAEs including minimisation criteria

Roland Pulch

Bergische Universität Wuppertal, Fachbereich Mathematik und Naturwissenschaften, Lehrstuhl für Angewandte Mathematik und Numerische Mathematik, Gaußstr. 20, D-42119 Wuppertal, Germany.

Abstract

Electric circuits, which produce oscillations at widely separated time scales, cause a huge computational effort in a numerical simulation of the mathematical model based on differential-algebraic equations (DAEs). Alternatively, a multidimensional signal model yields a description via multirate partial differential-algebraic equations (MPDAEs). Initial-boundary value problems of the MPDAE system reproduce solutions of the underlying DAE system. In case of frequency modulation, an additional function arises in the MPDAE model, which represents a degree of freedom in the multivariate description of the signals. We present two minimisation strategies, which are able to identify the additional parameters such that the resulting solutions exhibit an elementary structure. Thus numerical schemes can apply relatively coarse grids and an efficient simulation is achieved.

1 Introduction

Mathematical modelling of electric circuits applies a network approach, which generates systems of differential-algebraic equations (DAEs), see [3]. In many applications, signals acting at widely separated time scales arise. For example, fast oscillations may exhibit amplitude as well as frequency modulation, which are caused by slowly varying parts. Thus a numerical integration of the circuit's DAEs becomes inefficient, since the high-frequency oscillations limit the size of

time steps.

Alternatively, a multivariate signal model is able to decouple the time scales. Based on multivariate functions, Brachtendorf et al. [1] transformed the DAE system into multirate partial differential-algebraic equations (MPDAEs). Accordingly, a solution of the MPDAE system reproduces a solution of the underlying DAE system. Initial-boundary value problems or multiperiodic boundary value problems of the MPDAEs are considered to obtain corresponding solutions. The multidimensional approach has been successfully used for simulating circuits with amplitude modulated signals, see [9].

In case of frequency modulated signals, the model has to incorporate a local frequency function to achieve an efficient representation. Narayan and Roychowdhury [5] introduced a corresponding system of warped MPDAEs, which includes these parameters. Thereby, the local frequency function represents a degree of freedom in the modelling. Inappropriate choices cause many oscillations in the multivariate model and thus the strategy becomes inefficient. Hence additional conditions are necessary, which identify adequate local frequency functions.

An elementary approach consists in demanding continuous phase conditions, see [5]. Such additional constraints have been used successfully in time domain, see [6], as well as in frequency domain, see [10]. However, the phase conditions operate just in one component of the solution. Thus the idea is to impose minimisation demands, which guarantee an elementary structure in each component of the multivariate functions. Houben [4] constructed a strategy for solving initial-boundary value problems, where the amount of certain partial derivatives is minimised locally. On the other hand, a global minimisation criterion for determining multiperiodic solutions is introduced in [7].

In this paper, we present two strategies based on minimisation for solving initial-boundary value problems of the MPDAE system. The first approach is a direct generalisation of the technique given in [4], where a weighted norm is applied now. This strategy minimises the amount of certain partial derivatives corresponding to a charge term. Alternatively, the second technique demands a minimisation criterion for according derivatives of the solution itself. A necessary condition for an optimal solution results from a variational calculus with respect to transformation properties of solutions. We discuss advantages and disadvantages of both approaches. If the circuit's equations represent a system of ordinary differential equations (ODEs), then the two techniques are equivalent.

The paper is organised as follows. In Sect. 2, we sketch the multivariate signal model and the resulting MPDAE model. Thereby, required transformation properties of solutions are discussed. We derive the two minimisation criteria for identifying adequate solutions in Sect. 3. A numerical scheme based on a method

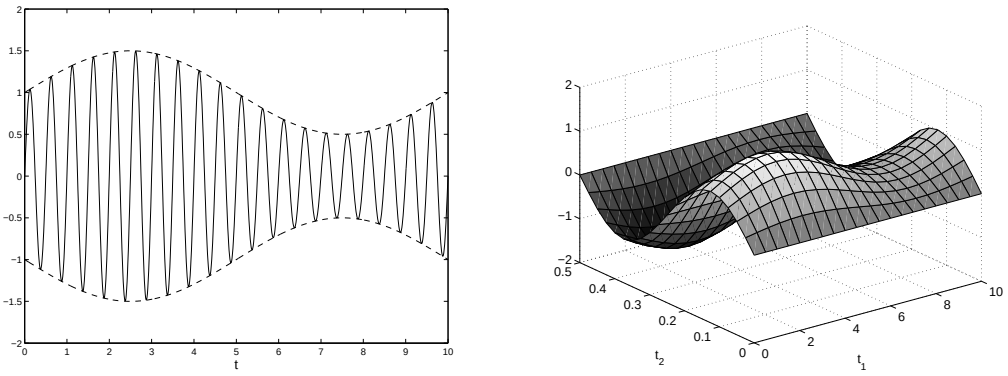

Figure 1: Amplitude modulated signal y (left) and corresponding MVF $\hat{y}$ (right).

of lines, which allows to include the conditions arising from the minimisation criteria, is constructed in Sect. 4. Finally, we present according numerical results using a modification of the Van-der-Pol oscillator.

2 MPDAE Model

We start with an outline of the multidimensional signal model. Firstly, we consider amplitude modulated signals. For example, the time-dependent function

$$y(t) := \left[1 + \alpha \sin\left(\tfrac{2\pi}{T_1} t\right)\right] \sin\left(\tfrac{2\pi}{T_2} t\right) \tag{1}$$

with $T_1 \gg T_2$ represents a high-frequency oscillation, where a fixed $\alpha \in (0, 1)$ introduces a modulation by a low-frequency oscillation, see Fig. 1 (left). Hence we require many time steps to resolve all oscillations in case of widely separated rates. Nevertheless, we can introduce an own variable for each time scale, which yields the formulation

$$\hat{y}(t_1, t_2) := \left[1 + \alpha \sin\left(\tfrac{2\pi}{T_1} t_1\right)\right] \sin\left(\tfrac{2\pi}{T_2} t_2\right). \tag{2}$$

This representation is called the *multivariate function* (*MVF*) of the signal (1). The MVF (2) is biperiodic and thus just determined by its values in the rectangle $[0, T_1] \times [0, T_2]$. Fig. 1 (right) illustrates that the MVF exhibits a simple structure. Hence a coarse grid in time domain is sufficient for resolving this representation. We can completely reconstruct the original signal (1) via $y(t) = \hat{y}(t, t)$. Hence we achieve an efficient multidimensional model of amplitude modulated signals.

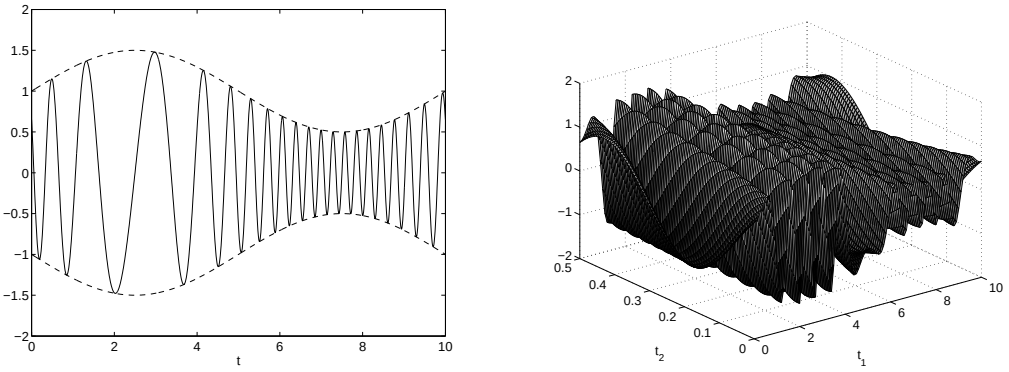

Figure 2: Frequency modulated signal x (left) and according MVF $\hat{x}_1$ using constant time rates (right).

Secondly, we examine signals, which include amplitude modulation as well as frequency modulation. In the signal

$$x(t) := \left[1 + \alpha \sin\left(\tfrac{2\pi}{T_1} t\right)\right] \sin\left(\tfrac{2\pi}{T_2} t + \beta \cos\left(\tfrac{2\pi}{T_1} t\right)\right), \tag{3}$$

the parameter $\beta > 0$ determines the amount of frequency modulation. Fig. 2 (left) demonstrates the signal qualitatively. We directly obtain a MVF by introducing separate variables for each time scale

$$\hat{x}_1(t_1, t_2) := \left[1 + \alpha \sin\left(\tfrac{2\pi}{T_1} t_1\right)\right] \sin\left(\tfrac{2\pi}{T_2} t_2 + \beta \cos\left(\tfrac{2\pi}{T_1} t_1\right)\right). \tag{4}$$

However, this biperiodic MVF exhibits many oscillations in the underlying rectangle, see Fig. 2 (right). The number of oscillations increases the larger the parameter β becomes. Thus the multidimensional model (4) is inefficient.

To obtain an adequate representation, Narayan and Roychowdhury [5] model just the amplitude modulation part via MVFs, whereas the frequency modulation part is described by an additional time-dependent function. For our signal (3), we obtain the MVF

$$\hat{x}_2(t_1, t_2) := \left[1 + \alpha \sin\left(\tfrac{2\pi}{T_1} t_1\right)\right] \sin\left(2\pi t_2\right), \tag{5}$$

where the second period is standardised to 1. This MVF exhibits the same elementary structure as the representation (2) illustrated in Fig. 1 (right). The frequency modulation is given by the *warping function*

$$\Psi(t) := \frac{t}{T_2} + \frac{\beta}{2\pi} \cos\left(\tfrac{2\pi}{T_1} t\right). \tag{6}$$

Now we reconstruct the underlying signal (3) using $x(t) = \hat{x}_2(t, \Psi(t))$, i.e. the warping function stretches the second time scale. The derivative of the warping function

$$\nu(t) := \Psi'(t) = \frac{1}{T_2} - \frac{\beta}{T_1} \sin\left(\tfrac{2\pi}{T_1} t\right) \tag{7}$$

can be seen as a *local frequency* of the signal (3). Thus we obtain an efficient model of frequency modulated signals applying MVFs and corresponding local frequency functions. However, the representation is not unique. For example, setting $\hat{x}_3(t_1, t_2) := \hat{x}_1(t_1, T_2 t_2)$ and $\Phi(t) := t/T_2$ yields $x(t) = \hat{x}_3(t, \Phi(t))$, too, where $\hat{x}_3$ is a $(T_1, 1)$-periodic MVF.

The above model is also applicable for signals, which are not periodic in the slow time scale. On the other hand, we always assume that the fast time scale has a periodic behaviour, which is necessary for the efficiency of the representation.

The mathematical model of electric circuits is based on a network approach, which yields systems of *differential-algebraic equations* (*DAEs*) for the transient behaviour of all node voltages and some branch currents, see [3]. We write the systems in the form

$$\frac{\mathrm{d}\mathbf{q}(\mathbf{x})}{\mathrm{d}t} = \mathbf{f}(\mathbf{x}(t)) + \mathbf{b}(t), \qquad \begin{aligned} \mathbf{x}, \mathbf{b} &: \ \mathbb{R} \to \mathbb{R}^k, \\ \mathbf{q}, \mathbf{f} &: \ \mathbb{R}^k \to \mathbb{R}^k, \end{aligned} \tag{8}$$

where $\mathbf{x}$ represents unknown voltages and currents. The function $\mathbf{q}$ describes charges as well as fluxes and $\mathbf{f}$ contains resistance terms. The function $\mathbf{b}$ includes independent input signals. We assume that the circuit produces high-frequency oscillations for constant input signals. Accordingly, a slowly varying input may cause amplitude and frequency modulation in these oscillations, i.e. the solution exhibits the time behaviour outlined above.

Thus the multidimensional signal model is applied for the function $\mathbf{x}$. The transition to MVFs changes the system of DAEs into a system of *multirate partial differential-algebraic equations* (*MPDAEs*). Following Narayan and Roychowdhury [5], the warped MPDAE corresponding to (8) reads

$$\frac{\partial \mathbf{q}(\hat{\mathbf{x}})}{\partial t_1} + \nu(t_1) \frac{\partial \mathbf{q}(\hat{\mathbf{x}})}{\partial t_2} = \mathbf{f}(\hat{\mathbf{x}}(t_1, t_2)) + \mathbf{b}(t_1). \tag{9}$$

Thereby, $\hat{\mathbf{x}} : \mathbb{R}^2 \to \mathbb{R}^k$ is the MVF of $\mathbf{x}$. The input signals vary just slowly and thus do not require a multivariate description. The local frequency $\nu : \mathbb{R} \to \mathbb{R}$ depends on the same variable as the input. It is straightforward to verify that the reconstruction

$$\mathbf{x}(t) := \hat{\mathbf{x}}\left(t, \int_0^t \nu(u)\, \mathrm{d}u\right) \tag{10}$$

using a solution of the MPDAE (9) yields a solution of the DAE (8).

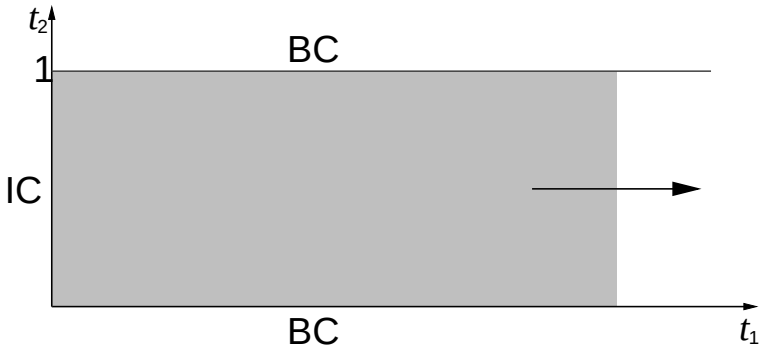

Figure 3: Initial-boundary value problem of the MPDAE.

To solve the MPDAE system, according boundary conditions have to be specified. The fast time scale is assumed to be periodic. Thus we consider the initial-boundary value problem

$$\hat{\mathbf{x}}(0, t_2) = \mathbf{h}(t_2), \quad \hat{\mathbf{x}}(t_1, t_2 + 1) = \hat{\mathbf{x}}(t_1, t_2) \quad \text{for all } \; t_1 \geq 0, \; t_2 \in \mathbb{R}, \tag{11}$$

where $\mathbf{h} : \mathbb{R} \to \mathbb{R}^k$ is a predetermined periodic function. Fig. 3 illustrates the problem in time domain. Using (10), a solution of the MPDAE satisfying (11) produces a solution of an initial value problem of the underlying DAE with $\mathbf{x}(0) = \mathbf{h}(0)$. Furthermore, if the slow time scale is periodic, too, then biperiodic boundary value problems of the MPDAE yield quasiperiodic responses of the corresponding DAE, cf. [6].

The MPDAE system (9) exhibits certain transformation properties, see [7]. If $\hat{\mathbf{x}}$ is a solution corresponding to a local frequency function ν, then the transformed MVF

$$\hat{\mathbf{y}}(t_1, t_2) := \hat{\mathbf{x}}\left(t_1, t_2 + \int_0^{t_1} \nu(u) - \mu(u) \, \mathrm{d}u\right) \tag{12}$$

satisfies the MPDAE system including the local frequency function μ. Initial conditions at $t_1 = 0$ are invariant in this transformation. The periodicity in the fast time scale is preserved, too. Moreover, both MVFs with their local frequency functions reproduce the same DAE solution using (10).

Since μ in (12) can be specified arbitrarily, we obtain a family of solutions satisfying the initial-boundary value problem (9),(11). Thus the local frequencies represent free parameters in the model. We want to identify frequency functions, which lead to adequate MVFs. In case of widely separated time scales, tiny changes in the local frequency function cause huge deformations in the corresponding MVF. Due to this sensitivity, we can not directly apply a predetermined specification of the frequency function. Alternatively, we have to impose

criteria on the corresponding MVF, which determine the local frequency function indirectly.

For specifying the unknown frequency function, we can try to control the phase in the cross sections of the MVF for each t_1. This approach yields phase conditions like

$$\hat{x}_1(t_1, 0) = \eta \quad \text{for all } \; t_1 \geq 0 \tag{13}$$

for an appropriate constant $\eta \in \mathbb{R}$ or

$$\frac{\partial \hat{x}_1}{\partial t_2}(t_1, 0) = 0 \quad \text{for all } \; t_1 \geq 0 \tag{14}$$

in the, without loss of generality, first component of the MVF $\hat{\mathbf{x}} = (\hat{x}_1, \ldots, \hat{x}_k)^\top$. Phase conditions have been successfully used in time domain, see [5, 6], as well as in frequency domain, see [10], to identify appropriate solutions in numerical simulations. The resulting MVFs exhibit a simple form, i.e. they do not contain unnecessary oscillations. However, since the phase conditions work only in a part of the solution, this advantageous property can not be guaranteed in general.

3 Minimisation Criteria

Observing Fig. 2 (right), we recognise that an inappropriate local frequency function causes many oscillations with respect to the slow time scale. Thus the idea is to reduce the number of oscillations by a minimisation of the amount of partial derivatives corresponding to the first time scale. An optimal solution ensures that we can use relatively large step sizes for solving the initial-boundary value problem (9),(11), when we proceed in the slow time scale.

We consider weights $w_1, \ldots, w_k \geq 0$ for each component. Consequently, we define the positive semi-definite, symmetric bilinear form

$$\langle \cdot, \cdot \rangle_{\mathrm{W}} : \mathbb{R}^k \times \mathbb{R}^k \to \mathbb{R}, \qquad \langle \mathbf{x}, \mathbf{y} \rangle_{\mathrm{W}} := \sum_{i=1}^{k} w_i \cdot x_i \cdot y_i. \tag{15}$$

The corresponding semi-norm reads

$$\| \cdot \|_{\mathrm{W}} : \mathbb{R}^k \to \mathbb{R}_0^+, \qquad \|\mathbf{x}\|_{\mathrm{W}} := \sqrt{\langle \mathbf{x}, \mathbf{x} \rangle_{\mathrm{W}}} = \left(\sum_{i=1}^{k} w_i \cdot {x_i}^2 \right)^{\frac{1}{2}}. \tag{16}$$

If all weights are positive, we obtain a positive definite form and an according norm. Setting $w_i = 1$ for all i yields the Euclidean norm. Choosing some weights

equal to zero allows to focus on an arbitrary subset of components. Furthermore, we can perform an appropriate scaling applying the weights, if the components exhibit different orders of magnitudes. In the following, we assume $w_i > 0$ for at least one i to achieve a non-trivial form.

Considering the initial-boundary value problem (9),(11), we want to minimise the amount of change in the slow time scale belonging to the points (t_1, t_2) for each fixed t_1 and all t_2. Due to the periodicity in the fast time scale, we define

$$\langle \cdot, \cdot \rangle_* : (L^2[0,1])^k \times (L^2[0,1])^k \to \mathbb{R}, \quad \langle \mathbf{x}, \mathbf{y} \rangle_* := \int_0^1 \langle \mathbf{x}(u), \mathbf{y}(u) \rangle_{\mathrm{W}} \, \mathrm{d}u, \tag{17}$$

which represents a positive semi-definite, symmetric bilinear form again. The resulting semi-norm shall be denoted by $\| \cdot \|_*$. Following Houben [4], we demand the minimisation criterion

$$s(t_1) := \left\| \frac{\partial \mathbf{q}(\hat{\mathbf{x}})}{\partial t_1}(t_1, \cdot) \right\|_*^2 \quad \longrightarrow \quad \min. \qquad \text{for each } \; t_1 \geq 0. \tag{18}$$

More precisely, since the function s depends on the MVF, we want to determine a solution $\hat{\mathbf{x}}$ satisfying (9),(11) for some local frequency, which fulfils

$$s(t_1; \hat{\mathbf{x}}) = \left\| \tfrac{\partial \mathbf{q}(\hat{\mathbf{x}})}{\partial t_1}(t_1, \cdot) \right\|_*^2 \leq \left\| \tfrac{\partial \mathbf{q}(\hat{\mathbf{y}})}{\partial t_1}(t_1, \cdot) \right\|_*^2 = s(t_1; \hat{\mathbf{y}}) \tag{19}$$

for each $t_1 \geq 0$ and all solutions $\hat{\mathbf{y}}$ of (9),(11) with their local frequencies. The requirement (18) involves only the derivative with respect to the slow time scale, since it holds

$$\left\| \tfrac{\partial \mathbf{q}(\hat{\mathbf{y}})}{\partial t_2}(t_1, \cdot) \right\|_*^2 = \left\| \tfrac{\partial \mathbf{q}(\hat{\mathbf{x}})}{\partial t_2}(t_1, \cdot) \right\|_*^2, \tag{20}$$

whenever $\hat{\mathbf{y}}$ and $\hat{\mathbf{x}}$ are connected by the transformation (12). We are able to replace the derivative in (18) by the other terms in the MPDAE (9) and achieve

$$\begin{aligned} s(t_1) &= \left\| \mathbf{f}(\hat{\mathbf{x}}(t_1, \cdot)) + \mathbf{b}(t_1) - \nu(t_1) \tfrac{\partial \mathbf{q}(\hat{\mathbf{x}})}{\partial t_2}(t_1, \cdot) \right\|_*^2 \\ &= \| \mathbf{f}(\hat{\mathbf{x}}(t_1, \cdot)) + \mathbf{b}(t_1) \|_*^2 + \nu(t_1)^2 \left\| \tfrac{\partial \mathbf{q}(\hat{\mathbf{x}})}{\partial t_2}(t_1, \cdot) \right\|_*^2 \\ &\quad - 2\nu(t_1) \langle \mathbf{f}(\hat{\mathbf{x}}(t_1, \cdot)) + \mathbf{b}(t_1), \tfrac{\partial \mathbf{q}(\hat{\mathbf{x}})}{\partial t_2}(t_1, \cdot) \rangle_*. \end{aligned} \tag{21}$$

An elementary minimisation calculus yields a necessary condition for an optimal local frequency function, namely

$$\nu(t_1) = \frac{\langle \mathbf{f}(\hat{\mathbf{x}}(t_1, \cdot)) + \mathbf{b}(t_1), \tfrac{\partial \mathbf{q}(\hat{\mathbf{x}})}{\partial t_2}(t_1, \cdot) \rangle_*}{\left\| \tfrac{\partial \mathbf{q}(\hat{\mathbf{x}})}{\partial t_2}(t_1, \cdot) \right\|_*^2} \qquad \text{for all } \; t_1 \geq 0. \tag{22}$$

Thereby, we assume that the denominator is not equal to zero for all $t_1 \geq 0$, which represents an insignificant constraint. Furthermore, the identification (22) is equivalent to the orthogonality relation

$$\langle \tfrac{\partial \mathbf{q}(\hat{\mathbf{x}})}{\partial t_1}(t_1,\cdot), \tfrac{\partial \mathbf{q}(\hat{\mathbf{x}})}{\partial t_2}(t_1,\cdot)\rangle_* = 0 \qquad \text{for all } \; t_1 \geq 0. \tag{23}$$

In case of positive weights, we remark that the MPDAE (9) can be transformed into an equivalent scaled system according to

$$\frac{\partial}{\partial t_1}\sqrt{w_i}\; q_i(\hat{\mathbf{x}}) + \nu(t_1)\frac{\partial}{\partial t_2}\sqrt{w_i}\; q_i(\hat{\mathbf{x}}) = \sqrt{w_i}\,(f_i(\hat{\mathbf{x}}(t_1,t_2)) + b_i(t_1)) \tag{24}$$

for $i = 1,\ldots,k$. Thus the above strategy corresponds to choosing the Euclidean norm in (16) for solutions of the MPDAEs (24).

A crucial advantage of this approach consists in the achievement of an explicit formula for the local frequency function. Thus we can insert (22) into the MPDAE (9) and obtain a well-determined system. However, the minimisation (18) is based on the charge term $\mathbf{q}(\hat{\mathbf{x}})$ and not on the MVFs $\hat{\mathbf{x}}$ itself. In general, the MVFs exhibit a low number of oscillations if and only if the corresponding charge term has the same property. Yet we can not guarantee this property. If the underlying system (8) represents a semi-explicit system of DAEs, then the minimisation criterion (18) involves no algebraic variable, i.e. algebraic variables can not be controlled.

Alternatively, we construct a minimisation criterion based on the partial derivatives of the MVFs itself, namely

$$p(t_1) := \left\| \frac{\partial \hat{\mathbf{x}}}{\partial t_1}(t_1,\cdot) \right\|_*^2 \quad \longrightarrow \quad \min. \qquad \text{for each } \; t_1 \geq 0. \tag{25}$$

The meaning of this demand is analogue to (19). To determine a necessary condition for an optimal solution, we perform a variational calculus using the transformation (12). Assume that $\hat{\mathbf{z}}$ is an optimal solution with respect to (25). Given an arbitrary smooth function $\Theta : \mathbb{R} \to \mathbb{R}$ with $\Theta(0) = 0$, we obtain a family of competitive solutions due to the transformations (12)

$$\hat{\mathbf{x}}_\varepsilon(t_1,t_2) := \hat{\mathbf{z}}(t_1, t_2 + \varepsilon\Theta(t_1)) \quad \text{for } \; \varepsilon \in \mathbb{R}. \tag{26}$$

The derivatives of the competitive functions read

$$\begin{aligned} \tfrac{\partial \hat{\mathbf{x}}_\varepsilon}{\partial t_1}(t_1,t_2) &= \tfrac{\partial \hat{\mathbf{z}}}{\partial t_1}(t_1, t_2+\varepsilon\Theta(t_1)) + \varepsilon\Theta'(t_1)\tfrac{\partial \hat{\mathbf{z}}}{\partial t_2}(t_1, t_2+\varepsilon\Theta(t_1)), \\ \tfrac{\partial \hat{\mathbf{x}}_\varepsilon}{\partial t_2}(t_1,t_2) &= \tfrac{\partial \hat{\mathbf{z}}}{\partial t_2}(t_1, t_2+\varepsilon\Theta(t_1)). \end{aligned} \tag{27}$$

In the following computations, we apply that

$$\langle \mathbf{x}(\cdot + c), \mathbf{y}(\cdot + c)\rangle_* = \langle \mathbf{x}(\cdot), \mathbf{y}(\cdot)\rangle_* \tag{28}$$

holds for all 1-periodic functions $\mathbf{x}, \mathbf{y} : \mathbb{R} \to \mathbb{R}^k$ and an arbitrary constant $c \in \mathbb{R}$. Consequently, we have

$$\begin{aligned} p(t_1;\varepsilon) &= \left\| \tfrac{\partial \hat{\mathbf{x}}_\varepsilon}{\partial t_1}(t_1,\cdot) \right\|_*^2 = \left\| \tfrac{\partial \hat{\mathbf{z}}}{\partial t_1}(t_1,\cdot) + \varepsilon \Theta'(t_1) \tfrac{\partial \hat{\mathbf{z}}}{\partial t_2}(t_1,\cdot) \right\|_*^2 \\ &= \left\| \tfrac{\partial \hat{\mathbf{z}}}{\partial t_1}(t_1,\cdot) \right\|_*^2 + \varepsilon^2 \Theta'(t_1)^2 \left\| \tfrac{\partial \hat{\mathbf{z}}}{\partial t_2}(t_1,\cdot) \right\|_*^2 \\ &\quad + 2\varepsilon \Theta'(t_1) \langle \tfrac{\partial \hat{\mathbf{z}}}{\partial t_1}(t_1,\cdot), \tfrac{\partial \hat{\mathbf{z}}}{\partial t_2}(t_1,\cdot) \rangle_*. \end{aligned} \tag{29}$$

Differentiation with respect to ε yields

$$\frac{\mathrm{d}p}{\mathrm{d}\varepsilon}(t_1;\varepsilon) = 2\varepsilon \Theta'(t_1)^2 \left\| \tfrac{\partial \hat{\mathbf{z}}}{\partial t_2}(t_1,\cdot) \right\|_*^2 + 2\Theta'(t_1) \langle \tfrac{\partial \hat{\mathbf{z}}}{\partial t_1}(t_1,\cdot), \tfrac{\partial \hat{\mathbf{z}}}{\partial t_2}(t_1,\cdot) \rangle_*. \tag{30}$$

Setting $\varepsilon = 0$ implies the relation

$$\Theta'(t_1) \langle \tfrac{\partial \hat{\mathbf{z}}}{\partial t_1}(t_1,\cdot), \tfrac{\partial \hat{\mathbf{z}}}{\partial t_2}(t_1,\cdot) \rangle_* = 0 \quad \text{for all } \ t_1 \geq 0. \tag{31}$$

Since this property has to be satisfied for arbitrary $\Theta \in C^1$ with $\Theta(0) = 0$, we may choose functions with $\Theta'(t_1) > 0$ for all $t_1 \geq 0$. Consequently, the necessary condition

$$\langle \tfrac{\partial \hat{\mathbf{z}}}{\partial t_1}(t_1,\cdot), \tfrac{\partial \hat{\mathbf{z}}}{\partial t_2}(t_1,\cdot) \rangle_* = 0 \quad \text{for all } \ t_1 \geq 0 \tag{32}$$

arises. This demand represents an orthogonality relation with respect to the bilinear form (17). Remark that we have not used the MPDAE system (9) directly to achieve the condition (32). We just applied the transformation formula (12), which results from the MPDAEs.

Concerning the existence of solutions satisfying the orthogonality relation (32), we achieve the following statement. Let $\hat{\mathbf{y}}$ be the solution of the initial-boundary value problem (9),(11) corresponding to local frequency $\nu \equiv 0$, which can be obtained by solving a family of initial value problems of the DAEs (8). Hence we define

$$\nu(t_1) := \frac{\langle \tfrac{\partial \hat{\mathbf{y}}}{\partial t_1}(t_1,\cdot), \tfrac{\partial \hat{\mathbf{y}}}{\partial t_2}(t_1,\cdot) \rangle_*}{\left\| \tfrac{\partial \hat{\mathbf{y}}}{\partial t_2}(t_1,\cdot) \right\|_*^2} \tag{33}$$

and according to (12)

$$\hat{\mathbf{z}}(t_1,t_2) := \hat{\mathbf{y}} \left(t_1, t_2 - \int_0^{t_1} \nu(u)\, \mathrm{d}u \right). \tag{34}$$

Thus $\hat{\mathbf{z}}$ is a solution of the MPDAE (9) corresponding to the local frequency ν, which exhibits condition (32). Consequently, if an arbitrary MPDAE solution satisfying (11) exists, then we achieve another solution, which fulfils (32). However, we do not know a reference solution a priori. Thus we have to determine the function ν indirectly by using the condition (32) in time domain.

If the underlying system (8) represents an ODE, i.e. $\mathbf{q}(\mathbf{x}) \equiv \mathbf{x}$, then the conditions (23) and (32) coincide. Accordingly, we obtain the identification (22), which we can apply to solve the initial-boundary value problem of the corresponding partial differential equations.

4 Numerical Method

Now we construct a numerical technique to obtain approximatively solutions of the above multidimensional approach. In [8], semidiscretisation methods are used to solve the initial-boundary value problem (11) of the MPDAEs (9) including phase conditions. Thereby, a method of lines as well as a technique of Rothe type are considered. Houben [4] applies also a method of lines to realise the minimisation via the necessary condition (22).

Likewise, we use a method of lines to include the alternative constraint (32). Hence we restrict the MVF in the MPDAE (9) to the lines

$$\tilde{\mathbf{x}}_j(t_1) \doteq \hat{\mathbf{x}}(t_1, (j-1)h_2) \quad \text{for } \; j = 1, \ldots, m \quad \text{with } \; h_2 := \tfrac{1}{m}. \tag{35}$$

Replacing the derivative of the fast time scale in (9) by a backward difference formula of second order, see [2], and considering the discretisation (35) yields the equations

$$\frac{\mathrm{d}\mathbf{q}(\tilde{\mathbf{x}}_j)}{\mathrm{d}t_1} = \mathbf{f}(\tilde{\mathbf{x}}_j) + \mathbf{b}(t_1) - \frac{\nu(t_1)}{h_2}\left[\frac{3}{2}\mathbf{q}(\tilde{\mathbf{x}}_j) - 2\mathbf{q}(\tilde{\mathbf{x}}_{j-1}) + \frac{1}{2}\mathbf{q}(\tilde{\mathbf{x}}_{j-2})\right] \tag{36}$$

for $j = 1, \ldots, m$. The periodicity condition in (11) allows for the identifications $\tilde{\mathbf{x}}_0 = \tilde{\mathbf{x}}_m$ and $\tilde{\mathbf{x}}_{-1} = \tilde{\mathbf{x}}_{m-1}$. Thus the systems (36) represent mk DAEs for the mk unknown approximations (35). Furthermore, we apply a discretisation of the relation (32) according to the structure of the lines. The derivative of the fast time scale is substituted by a difference formula of first order and the integral is replaced by a finite sum. Numerical simulations show that a discretisation of the additional condition (32) does not require a higher accuracy, i.e. rough approximations are sufficient. Consequently, the relation

$$\begin{aligned} 0 \;=\; \langle \tfrac{\partial \hat{\mathbf{x}}}{\partial t_1}(t_1,\cdot), \tfrac{\partial \hat{\mathbf{x}}}{\partial t_2}(t_1,\cdot)\rangle_* \;&=\; \sum_{l=1}^{k} w_l \int_0^1 \tfrac{\partial \hat{x}_l}{\partial t_1}(t_1,u) \cdot \tfrac{\partial \hat{x}_l}{\partial t_2}(t_1,u)\,\mathrm{d}u \\ &\doteq\; \sum_{l=1}^{k} w_l \sum_{j=1}^{m} \tfrac{\mathrm{d}\tilde{x}_{j,l}}{\mathrm{d}t_1}(t_1) \cdot [\tilde{x}_{j,l}(t_1) - \tilde{x}_{j-1,l}(t_1)]\,. \end{aligned} \tag{37}$$

arises for $\tilde{\mathbf{x}}_j = (\tilde{x}_{j,1}, \ldots, \tilde{x}_{j,k})^\top$. This condition exhibits the structure of a scalar function depending on t_1, which can be used to determine the local frequencies for

each t_1. In the discretised form, just terms depending on the unknown approximations (35) are included. Thus we add the relation (37) to the systems (36). The required initial values for the approximative systems (36) follow from (11). Now we can solve the total system (36),(37) by proceeding in the slow time scale. Thereby, the derivatives with respect to the slow time scale, which arise in (36) as well as (37), have to be discretised further.

5 Illustrative Example

To demonstrate our technique, we consider a modification of the Van-der-Pol oscillator. The corresponding system reads

$$\begin{aligned} \dot{x}_1 &= x_2 \\ \dot{x}_2 &= -10({x_1}^2 - 1)x_2 - 4\pi^2 x_1 + A\sin\left(\tfrac{2\pi}{T}t\right) \\ 0 &= x_1 + {x_3}^3 + 3, \end{aligned} \tag{38}$$

which represents a semi-explicit DAE of index 1. In the input signal, we choose the amplitude $A = 30$ and the time rate $T = 1000$. If $A = 0$ holds, then the DAE (38) exhibits a periodic solution with frequency $\nu_0 \approx 1$. On the other hand, frequency modulation at widely separated time scales arises in case of $A \neq 0$. Consequently, we change to the according warped MPDAE system (9), where it holds

$$\mathbf{q}(\hat{\mathbf{x}}) \equiv \mathbf{q}(x_1, x_2, x_3) \equiv (x_1, x_2, 0)^\top. \tag{39}$$

Simulations of biperiodic problems for the ordinary Van-der-Pol oscillator as an ODE system ($\mathbf{q}(\hat{\mathbf{x}}) \equiv \hat{\mathbf{x}}$) are performed in [6].

We consider the initial-boundary value problem (9),(11) in the following. As starting values, we employ a periodic solution of (38) from the case $A = 0$. Firstly, we determine a solution of the MPDAEs using the phase condition (13) with $\eta = 0$. Secondly, the necessary condition (32) is applied to obtain an optimal solution. We choose the weights $w_1 = 1, w_2 = 0.1, w_3 = 1$ due to the different magnitudes of the components. In both simulations, we consider the systems (36) resulting from the method of lines. Firstly, the phase condition (13) is added directly. Secondly, we apply the discretised formulation (37). Then each initial value problem of a DAE system is integrated using the implicit Euler scheme.

Fig. 4 illustrates the achieved local frequency functions. The difference between the two results is relatively small ($|\nu_{\mathrm{opt}} - \nu_{\mathrm{ph}}| < 10^{-3}$). The corresponding MVFs are shown in Fig. 5. We recognise that all MVFs exhibit a simple behaviour, where a low number of oscillations arises. The second component $\hat{x}_2$ features a larger amount of amplitude modulation in comparison to the first component $\hat{x}_1$.

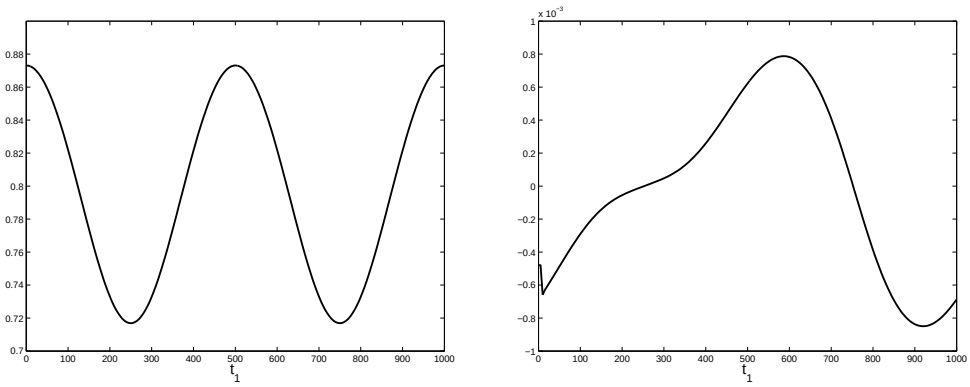

Figure 4: Local frequency function ν_{opt} (left) obtained from optimality criterion and difference $\nu_{\text{opt}} - \nu_{\text{ph}}$ (right), where ν_{ph} corresponds to the phase condition.

The algebraic component $\hat{x}_3$ is similar to $\hat{x}_1$. Although the differences between the local frequency functions ν_{opt} and ν_{ph} are tiny, we observe a significant difference in the MVFs. This fact indicates the said sensitivity in case of widely separated time scales.

To discuss the used minimisation criterion, we evaluate approximately the function (25) for both solutions. Fig. 6 demonstrates resulting approximations. Indeed, the solution corresponding to the minimisation demand (32) exhibits a smaller or equal amount than the solution with the phase condition (13). Hence larger step sizes with respect to the slow time scale can be applied to compute the optimal solution in a method of lines. Nevertheless, the amount of growth is not seriously larger in case of the phase condition. Thus phase conditions yield efficient solutions in this example, too.

Consequently, we reconstruct corresponding solutions of the DAEs (38) via (10) using the solution of the MPDAEs based on the optimality criterion. For comparison, we solve an initial value problem of the DAEs (38) via backward difference formulae, see [2], where we apply the initial value $\mathbf{x}(0) := \mathbf{h}(0)$ from (11). The results belonging to the first component x_1 are illustrated for two different time intervals by Fig. 7. In the first few cycles, the two signals exhibit a good agreement. In later cycles, a phase shift occurs, since small numerical errors in the local frequency function amplify during many oscillations. Moreover, transient integrations of the DAEs (38) produce a phase shift in comparison to the exact solution, too. Nevertheless, the other properties of the signal agree in later cycles, i.e. the shape, the amplitude and the frequency. Likewise, the components x_2 and x_3 exhibit the same behaviour. Using the MPDAE solution with the phase condition yields nearly the same signal as for the presented reconstruction. Thus

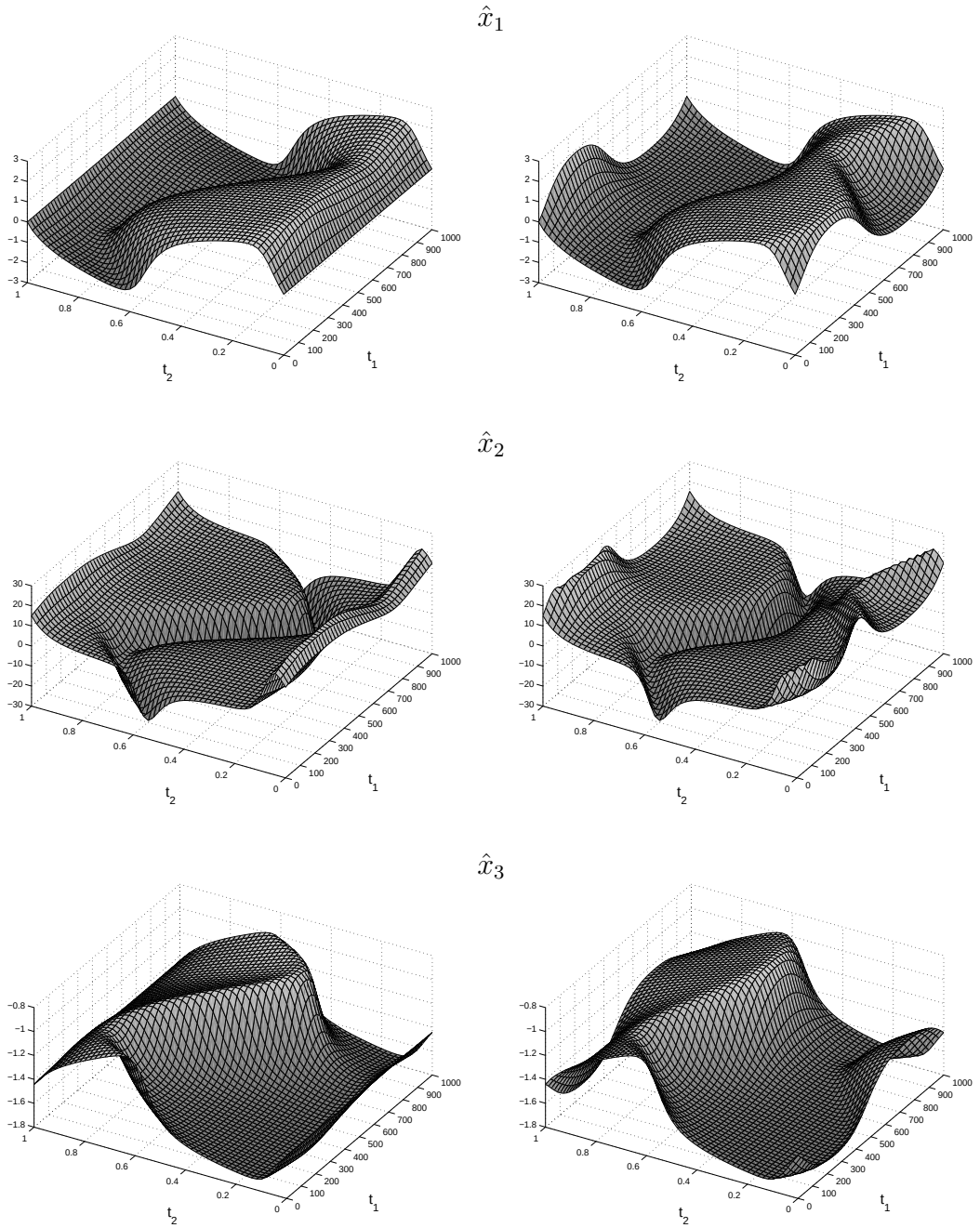

Figure 5: MVFs $\hat{x}_1, \hat{x}_2, \hat{x}_3$ resulting from phase condition (left) and from optimality criterion (right).

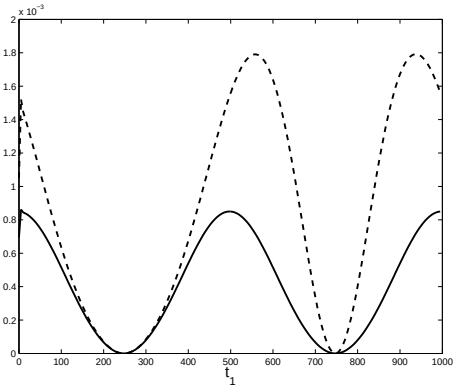

Figure 6: Function (25) evaluated at solution from minimisation criterion (solid line) and at solution from phase condition (dashed line).

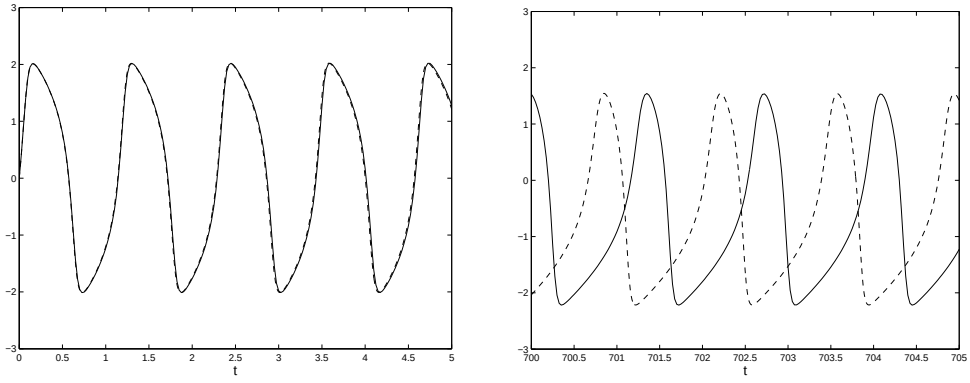

Figure 7: Solution x_1 of the DAE system (38) reconstructed from MPDAE solution (solid line) and achieved by transient integration (dashed line) in time intervals $[0, 5]$ (left) and $[700, 705]$ (right).

the MPDAE model considering initial-boundary value problems achieves a higher accuracy in phase compared to a numerical integration of underlying DAEs. This property is reported in [5], too.

Finally, we want to compare different weightings in the optimality criterion (25). Hence we perform the above numerical simulation again using several choices of weights. Unfortunately, there is no universal criterion for comparing the efficiency of different multivariate representations. Thus we use the function p in (25) for evaluating the computed solutions, too, with $w_1 = 1$, $w_2 = 0.1$, $w_3 = 1$ in any case now. The results yield an approximation of the mean value

$$\bar{p} := \frac{1}{T} \int_0^T p(u) \, \mathrm{d}u. \tag{40}$$

Table 1: Values of critical function for different approaches.

	approach	mean $\bar{p}$
(i)	phase condition	$8.5766 \cdot 10^{-4}$
(ii)	$w_1 = 1, w_2 = 0.1, w_3 = 1$	$4.0914 \cdot 10^{-4}$
(iii)	$w_1 = 1, w_2 = 1, w_3 = 0$	$4.0917 \cdot 10^{-4}$
(iv)	$w_1 = 1, w_2 = 0, w_3 = 0$	$4.2228 \cdot 10^{-4}$
(v)	$w_1 = 0, w_2 = 1, w_3 = 0$	$4.0918 \cdot 10^{-4}$
(vi)	$w_1 = 0, w_2 = 0, w_3 = 1$	$4.5760 \cdot 10^{-4}$

Table 1 demonstrates the determined mean values for different weighting techniques. Case (i) corresponds to the solution satisfying the phase condition. Case (iii) is equivalent to Houben's approach (18) using the Euclidean norm in (16). The best results are obtained in case (ii), since the used weights in the optimisation (25) as well as in the following evaluation of (40) coincide.

In our example, we conclude that the representation of one component is efficient if and only if the representation of all components is suitable. Moreover, the values of (40) seem to be dominated by the behaviour of the second component $\hat{x}_2$, because the MVF includes steep gradients. In other applications, the components may exhibit a different behaviour from each other. Accordingly, an optimisation using (25) based on all components, i.e. all weights are positive, achieves a tradeoff. Remark that a minimisation with respect to the algebraic component $\hat{x}_3$ is not feasible, if the alternative demand (18) is used.

6 Conclusions

A multivariate signal model transforms the circuit's DAEs into MPDAEs, where a local frequency function represents a degree of freedom. Considering initial-boundary value problems, two conditions to determine adequate local frequency functions have been presented, which both follow from minimisation criteria. The first approach yields an explicit formula for the local frequencies. The second approach imposes an additional condition on the multivariate functions, but allows more flexibility. If the circuit's equations represent ODEs, the two strategies are equivalent. The MPDAEs including the minimisation procedures can be solved approximately via a method of lines. Numerical simulations demonstrate that both techniques identify appropriate solutions.

References

[1] Brachtendorf, H. G.; Welsch, G.; Laur, R.; Bunse-Gerstner, A.: Numerical steady state analysis of electronic circuits driven by multi-tone signals. Electrical Engineering 79 (1996), pp. 103-112.

[2] Gear, C.W.: Simultaneous numerical solution of differential-algebraic equations. IEEE Trans. on Circuit Theory 18 (1971), pp. 89–95.

[3] Günther, M.; Feldmann, U.: CAD based electric circuit modeling in industry I: mathematical structure and index of network equations. Surv. Math. Ind. 8 (1999), pp. 97-129.

[4] Houben, S.H.M.J.: Simulating multi-tone free-running oscillators with optimal sweep following. In: Schilders, W.H.A., ter Maten, E.J.W., Houben, S.H.M.J. (eds.): Scientific Computing in Electrical Engineering, Mathematics in Industry 4, Springer, Berlin, 2004, pp. 240-247.

[5] Narayan, O.; Roychowdhury, J.: Analyzing oscillators using multitime PDEs. IEEE Trans. CAS I 50 (2003) 7, pp. 894-903.

[6] Pulch, R.: Multi time scale differential equations for simulating frequency modulated signals. Appl. Numer. Math. 53 (2005) 2-4, pp. 421-436.

[7] Pulch, R.: Variational methods for solving warped MPDAEs. Preprint BUW-AMNA 05/01, University of Wuppertal (2005).

[8] Pulch, R.: Semidiscretisation methods for warped MPDAEs. In: Anile, A.M.; Alì, G.; Mascali, G. (eds.): Scientific Computing in Electrical Engineering. Mathematics in Industry 9, Springer, Berlin, 2006, pp. 101-106.

[9] Roychowdhury, J.: Analysing circuits with widely-separated time scales using numerical PDE methods. IEEE Trans. CAS I 48 (2001) 5, pp. 578-594.

[10] Zhu, L. L.; Christoffersen, C. E.: Fast transient analysis of oscillators using multiple time scales with accurate initial conditions. IEEE Canadian Conference on Computer and Electrical Engineering Digest, Saskatoon, May 2005, pp. 700-703.